COMSOL
CONFERENCE
2024 FLORENCE

Modelling of Ink Jet Breakup using COMSOL Multiphysics®

F. Viry[1], M. Sturma[2], P. Namy[1], B. Barbet[2].

1. SIMTEC, Grenoble, France.

2. MARKEM-IMAJE, Bourg-lès-Valence, France.

Abstract

Continuous inkjet technology is widely used in the industry for marking and coding, and reposes on the emission of charged droplets at high velocity and high frequency. The shape of the droplets and the length needed for jet breakup are significant factors in the design of a printhead, influencing both the apparatus size and the printing quality. Understanding how the geometry of the droplet generator, the ink properties, and the operating point impact these indicators is then of prime importance. This article presents a modelling approach to the ink jet breakup process using COMSOL Multiphysics®.

The model represents the geometry of the nozzle, and the ink-air mixture downstream in 2D-axisymmetry. The diphasic flow is laminar, and is modelled using the Laminar Flow interface, coupled with the level-set method. The generation and perturbation of the ink jet are controlled using a periodic positive pressure drop, from upstream to downstream of the nozzle. The transient flow is solved until a periodic solution is found. The novelty of this work is the use of a Navier-slip boundary condition at walls, allowing to stack all process uncertainties. Once the slip parameter is fitted, this method enables an accurate prediction of the ink jet breakup in multiple configurations. The model can then be used to predict the shape of the droplets and the breakup length of new configurations, which may save weeks of experimental work.

Keywords: Continuous inkjet printing, industrial printer, CFD, two-phase flow, level-set method, ink-air interaction, Rayleigh-Plateau instability, slipping conditions, Navier-slip.

1 Introduction

The continuous inkjet technology (CIJ) is widely used in industrial marking and coding. The process consists in emitting and charging droplets of small size (typically 100 µm of diameter) at high-frequency (typically 100 kHz) and high velocity (typically 20 m/s), then deflecting them through an intense electric field, such that the droplets land at specific positions on the printed surface. By adjusting the electric charge embedded within each droplet, their final position is controlled. The shape of the generated droplets has a direct impact on the printing quality, as it directly impacts the ability to control the charges. Understanding the droplet generation process and having numerical tools to predict the droplet shapes is then of prime importance to overcome one the main challenges of the CIJ technology: printing as fast as possible while maintaining a certain level of printing quality.

In a droplet generator, a continuous ink flow pass through a stimulation chamber, where a piezoelectric membrane applies a periodic pressure perturbation, and a nozzle, downstream which an ink jet develops in ambient air at high velocity. The pressure perturbation transforms into a growing radius perturbation along the jet, which breaks at some distance to the nozzle thanks to the Rayleigh-Plateau instability. Depending on the droplet generator geometry, the ink properties, and the stimulation operating point, various droplet shapes and breakup lengths (distance between the nozzle and the just formed droplet) can be obtained. In [1], a diphasic CFD model was proposed to model how the periodic pressure stimulation upstream the nozzle develops along the jet in ambient air. In [2], the authors proposed an evolution of this latter model to study and predict liquid tin droplet formation for the extreme ultraviolet lithography technology. In our previous work [3], we redeveloped the model proposed in [1] in COMSOL Multiphysics®, and promising results were obtained in terms of droplet shape prediction for some configurations, while many others stayed unpredicted, indicating that an ingredient may be missing in the model. Finally, in [4], the authors proposed a simple numerical model to predict the well-known non-monotonic behavior of the breakup length in function of the stimulation amplitude, but the model cannot predict droplet shapes.

This article aims to improve the predictive capabilities of the model developed in [3] by replacing the no-slip boundary condition on the droplet generator walls into a Navier-slip boundary condition. This boundary condition introduces a new degree of freedom, and the article proposes a method to optimize this parameter such that most of the

experimental results can be predicted with high accuracy.

2 Experimental Setup

In the experimental test bench, a regulated mean ink flow supplies the droplet generator. The periodic pressure stimulation amplitude produced by the piezoelectric membrane within the droplet generator is controlled *via* a high-frequency voltage signal. Snapshots of the formed jet are optically captured thanks to a stroboscopic light at the same frequency than the perturbation signal. The process is periodic, and different snapshots can be selected by controlling the phase shift of the stroboscope.

During one period of the process, the jet length, which is the length of the continuous part of the ink jet from the nozzle, increases until a droplet forms and detaches from the jet. Once the jet breaks, the jet length suddenly decreases. At the exact instant where the jet splits into a smaller jet and a droplet: the jet length is called the *breakup length* L_b, and the shape of the jet is called the *jet shape at breakup*.

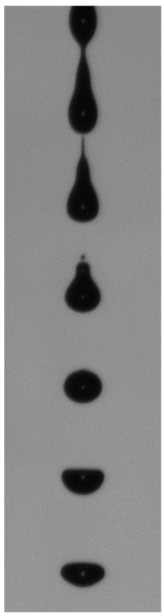

Figure 1. Example of experimental snapshot of the jet at breakup.

A large experimental campaign has been conducted to gather data on the process for multiple nozzle geometries, ink formulations, and stimulation frequencies. For each experiment, many perturbation signal amplitude V_{piezo} values are applied, and multiple indicators are tracked:

- Volumetric mean flow Q, known by mass measurement;
- Jet velocity v_{jet}, defined as the velocity of the just formed droplets, obtained by measuring the wavelength (center-to-center droplets distance), multiplied by the stimulation frequency;
- Breakup length L_b;
- Snapshot of the jet shape at breakup, as illustrated in Figure 1.

It has been shown experimentally that Q and v_{jet} do not depend on V_{piezo}.

3 Numerical Model

The aim of the model is to quantify the effect of the geometry of the nozzle, the ink properties, and the stimulation operating point, on the breakup length and the droplet shapes.

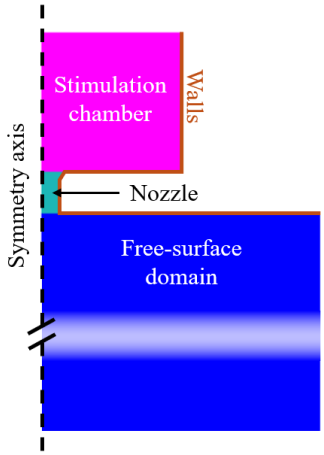

Figure 2. Schematic representation of the computational domain.

The computational domain is 2d-axysymetric, and is composed of the concatenation of the stimulation chamber (a cylinder), the nozzle (a cylinder with a specific chamfer), and the free-surface domain (a cylinder) long enough to contain a few formed droplets, as pictured in Figure 2. The two-phase flow (ink and air) is modelled by coupling incompressible Navier-Stokes equations with the Level-set method. The ink properties appearing in these equations are the density ρ, the dynamic viscosity μ and the ink-air surface tension σ. At the top of the stimulation chamber, an oscillatory pressure is imposed:

$$p = p_0 + p_1 \cdot \sin(2\pi\, f_{jet}\, t) \qquad (1)$$

where p_0 controls the mean ink flow, p_1 controls the perturbation amplitude, and f_{jet} is the stimulation frequency. The outer boundaries of the free-surface domain are set as open boundaries with $p = 0$. A more detailed description of the model and its numerical aspects is given in [3].

The main contribution of this work is using a Navier-slip boundary condition at the walls. This boundary condition prescribes a no-penetration

condition, but allows the velocity to be non-zero at the walls by imposing that the shear viscous stress is proportional to the velocity:

$$[K\boldsymbol{n} - (K\boldsymbol{n}) \cdot \boldsymbol{n}]\, \boldsymbol{n} = -\frac{\mu}{\beta_{NS}}\boldsymbol{u} \qquad (2)$$

where K is the viscous stress tensor, $\boldsymbol{n}$ is the wall normal, μ is the ink dynamic viscosity, $\boldsymbol{u}$ is the ink velocity, and β_{NS} is a parameter controlling the degree of slip. At the limits, when $\beta_{NS} \to \infty$, this condition becomes equivalent to the classical slip condition, while when $\beta_{NS} \to 0$, this condition behaves like a classical no-slip condition. This boundary condition provides a new degree of freedom and becomes a mean to consider uncertainties in friction forces at the walls due to milling geometrical tolerances, presence of rugosities, non-newtonian behavior of inks… *etc.*

This model is CFD only, so that some parameters have to be finely adjusted to reproduce physical experiments. The three parameters to adjust are: p_0, the mean ink pressure difference between upstream and downstream the nozzle, p_1 the perturbation amplitude obtained by the piezoelectric membrane with a signal of amplitude V_{piezo}, and β_{NS}, the Navier-slip condition parameter. It has to be noted that the model reproduces the same behavior than the experiments: the mean volumetric flow and the jet velocity are independent of p_1. Thus, parameters p_0 and β_{NS} are adjusted altogether such that the numerical volumetric mean flow and the numerical jet velocity equal the experimental values, and then, simulations are performed with multiple values of p_1. The law of the piezoelectric membrane $p_1 \leftrightarrow V_{piezo}$ is then determined by comparing numerical and experimental breakup lengths.

4 Results and Discussion

The numerical model is compared to physical measurements obtained in two experiments. For both experiments, the nozzle geometry and the operating point are typical of CIJ printing applications. The ink composition varies between experiments, and particularly their viscosities. These viscosity variations are typical consequences of ambient temperature variations, and it becomes very interesting to evaluate the predictive capabilities of the model subjected to such variations. For both experiments, the numerical parameters p_0 and β_{NS} have been adjusted as described in Section 3. The results are given in function of the perturbation amplitude.

Results of Experiment 1: Low Viscosity

The experimental and numerical jet shapes at breakup are given in Figure 3, and the breakup lengths are given in Figure 4.

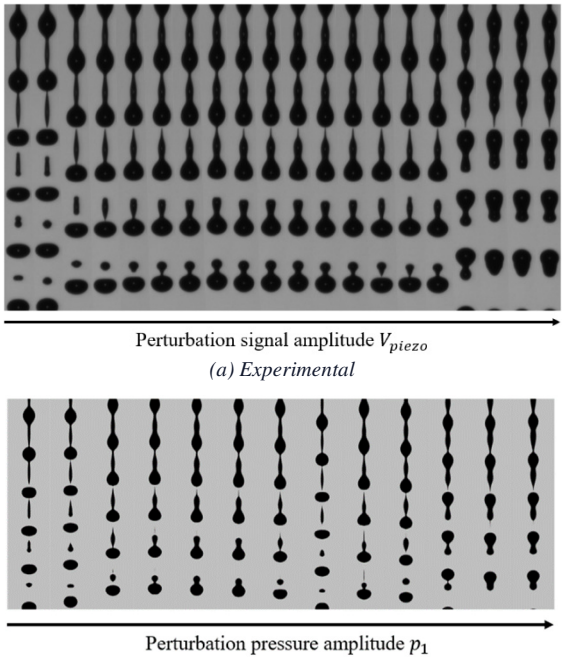

(a) Experimental

(b) Numerical

Figure 3. Low viscosity - jet shapes at breakup.

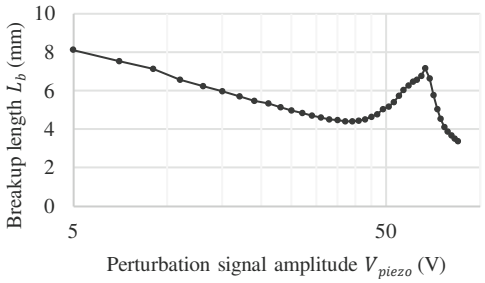

(a) Experimental

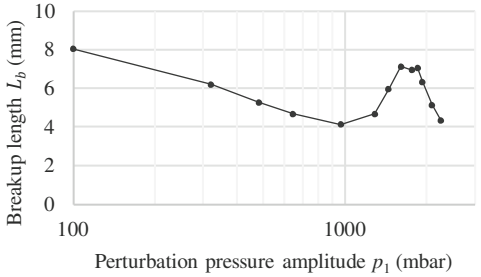

(b) Numerical

Figure 4. Low viscosity - breakup lengths.

Results of Experiment 2: High Viscosity

The experimental and numerical jet shapes at breakup are given in Figure 5, and the breakup lengths are given in Figure 6.

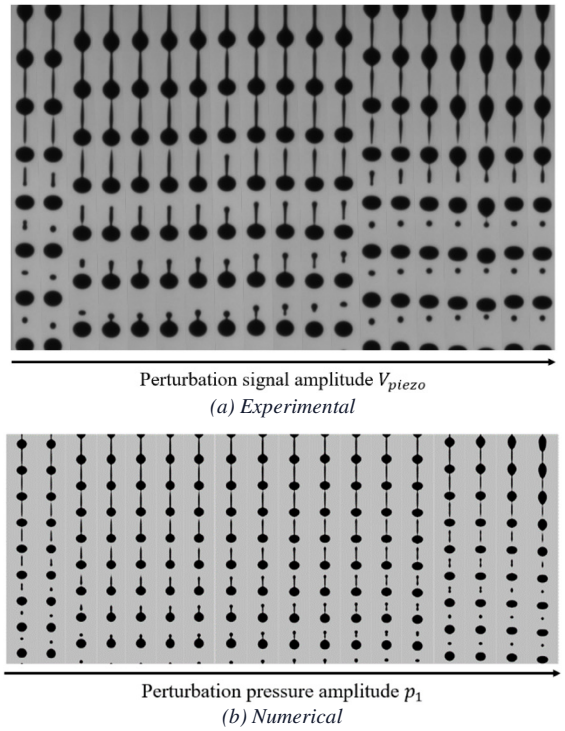

(a) Experimental

(b) Numerical

Figure 5. High viscosity - jet shapes at breakup.

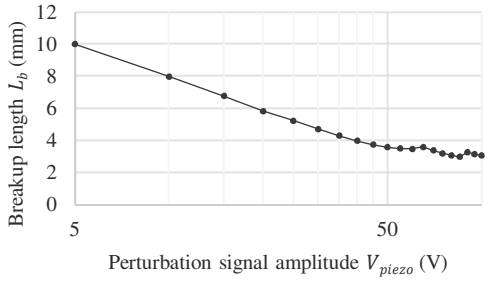

(a) Experimental

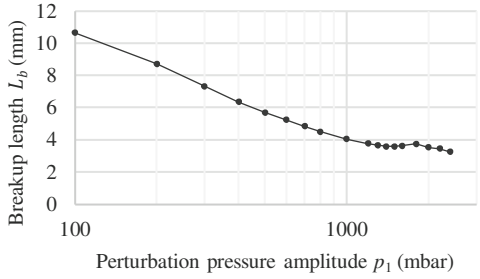

(b) Numerical

Figure 6. High viscosity - breakup lengths.

Predictive Capabilities of the Model

The numerical results look very close to experimental ones, both for the jet shapes at breakup, and the breakup lengths. In order to compare quantitatively the model and experiments, a law must be found between the experimental perturbation signal amplitude V_{piezo} and the numerical perturbation pressure amplitude p_1. For that, the model and experimental breakup length curves are fitted as best by assuming a linear relationship between V_{piezo} and p_1. A linear relationship is justified for small perturbation amplitude, while when the perturbation amplitude is high, nonlinearities may occur. The best linear relationships are illustrated in Figure 7, and the results are very satisfying: the slope at low perturbation amplitudes and the non-monotonic behavior observed at high perturbation amplitudes (specifically for the low viscosity experiment) are very accurately predicted.

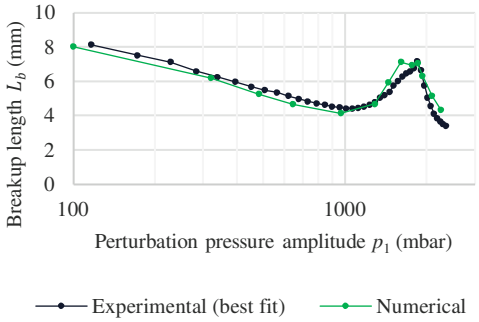

(a) Experiment 1: low viscosity

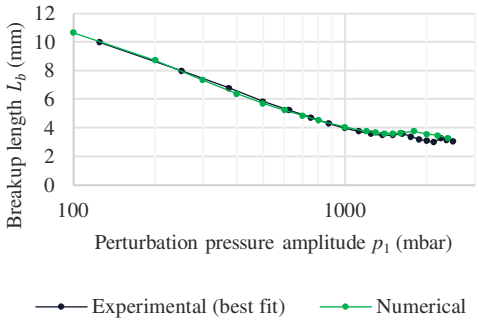

(b) Experiment 2: high viscosity

Figure 7. Results of the breakup length curve fitting.

Concerning the predictive capabilities of the jet shapes at breakup, experimental and numerical results can now be compared, given the relationship between V_{piezo} and p_1. In Figure 8, all experimental jet shapes at breakup are represented, superposed by numerical jet shapes at breakup obtained at the closest equivalent perturbation pressure amplitude. Numerical jet shapes at breakup that cannot be

correlated with an experimental one are not represented.

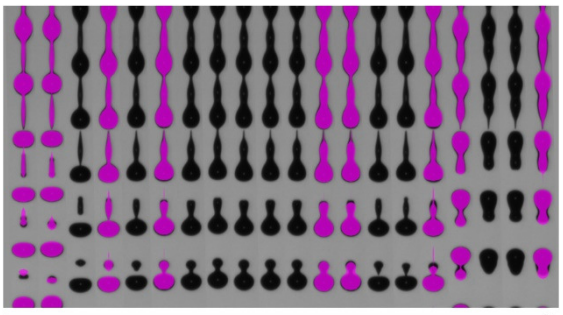

(a) Experiment 1: low viscosity

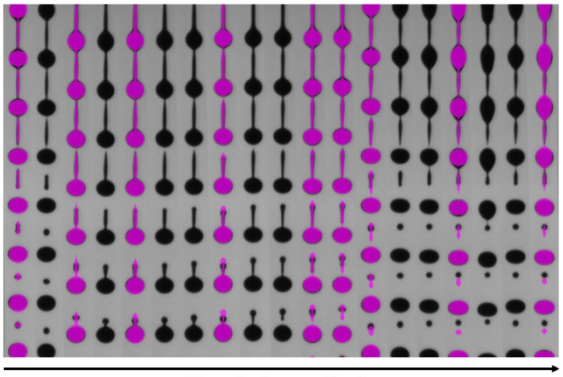

(b) Experiment 2: high viscosity

Figure 8. Comparison of jet shapes at breakup. Numerical shapes (in magenta) are superposed over experimental pictures (black and grey).

Globally, all the types of jet shapes at breakup observed experimentally are predicted by the model, as pictured in Figure 8. There are slight differences in the dynamics of satellites (secondary droplets), especially for Experiment 2 (high viscosity), but the presence or the absence of these satellites is correctly predicted. A small part of the types of numerical jet shapes at breakup predicted by the model, appearing in Figure 3 and Figure 5, are not present in Figure 8: these are the few cases where the model predicts a shape that has never been observed experimentally. These cases appear especially in the non-monotonic breakup length zone pictured in Figure 4 for Experiment 1 (low viscosity), which is out of the operating range exploited in CIJ printing.

Thus, the numerical model can be stated as predictive: three numerical parameters have been adjusted, allowing to predict a large number of breakup lengths and jet shapes at. To our knowledge, our work is the first to propose a numerical model capable to predict these indicators on such a large range of perturbation amplitudes. Next steps include understanding the causes of slipping at walls (non-newtonian behavior of inks, effect of rugosities... *etc*), and modelling the piezoelectric membrane to get a more physically-based prediction of the relationship between V_{piezo} and p_1. These improvements will help to limit the use of experimental data to calibrate the model.

5 Conclusions

In CIJ printing, controlling accurately were droplets form and their shape at breakup is of prime importance to ensure a certain printing quality. Having numerical tools to predict accurately the jet breakup phenomenon may save weeks of experimental work, and would open doors for numerical optimization.

The novelty of this work is improving an existing two-phase numerical model of the jet formation and breakup, by proposing the use of a new boundary condition at walls (Navier-slip), and a method to calibrate the model using experimental data. Once the three unknown parameters are adjusted, the numerical model predicts very accurately the breakup lengths and the jet shapes at breakup on multiple configurations representative of industrial operating conditions, on a larger range than existing works.

Future works include adding more features to the model (rheological law of inks, effect of rugosities, modelling the piezoelectrical membrane) to reduce the dependence to experimental data.

References

[1] M. Rosello, Etudes numérique et expérimentale de l'instabilité de Rayleigh-Plateau : Application aux jets d'encres, PhD Thesis, Université Grenoble Alpes, 2017.

[2] Z. Zhao and W. Li, "Numerical study of continuous liquid tin jet breakup and satellite droplet formation," *AIP Advances,* vol. 12, no. 125216, pp. 1-11, 2022.

[3] M. Sturma, A. Monlon, P. Namy, F. Viry and B. Barbet, "Modelling of Droplet Charge Dynamics during an Ink Jet Breakup using COMSOL Multiphysics®," in *COMSOL Conference*, Munich, 2023.

[4] T. Otowa, S. Tsubouchi and Y. Suwa, "Analysic of the Ink-Stream Break-up Phenomenon in Continuous Inkjet Printing," *ACS Omega,* vol. 8, no. 38, pp. 34442-34447, 2023.

Acknowledgements

This work has been founded by MARKEM-Imaje and made in a fruitful collaboration between MARKEM-Imaje and SIMTEC.